Title
EVIDENCE OP INCOMPLETE RELAXATION IN THE REACTION Ag + 30Ar AT 288 and 340 Mev BOMBARDING ENERGIES

Author
Galin, J.

Publication Date
1975-07-01

Submitted to Nuclear Physics

LBL-4064
Preprint

EVIDENCE OF INCOMPLETE RELAXATION IN THE REACTION Ag + ^{40}Ar AT 288 AND 340 Mev BOMBARDING ENERGIES

J. Galin, L. G. Moretto, R. Babinet, R. Schmitt,
R. Jared, and S. G. Thompson

July 1975

Prepared for the U. S. Energy Research and
Development Administration under Contract W-7405-ENG-48

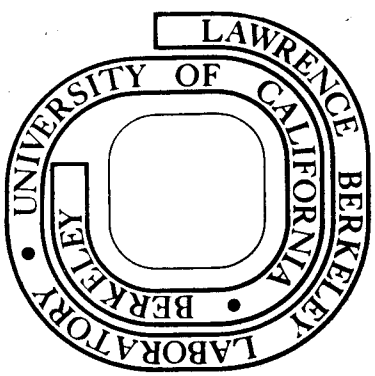

DISCLAIMER

LBL-4064

EVIDENCE OF INCOMPLETE RELAXATION IN THE REACTION Ag + ^{40}Ar AT 288 AND 340 Mev BOMBARDING ENERGIES*

J. Galin†, L. G. Moretto ‡, R. Babinet¶,

R. Schmitt, R. Jared and S. G. Thompson

Department of Chemistry

and

Lawrence Berkeley Laboratory

University of California

Berkeley, California 94720

ABSTRACT

The particles emitted in the reaction induced by ^{40}Ar on natural Ag at 288 and 340 Mev bombarding energy have been studied. The fragments have been identified in atomic number, their kinetic energy distribution and their angular distributions have been measured. The kinetic energy spectra show two components: a high energy component related to the beam energy, or "quasi elastic" component, and a low kinetic energy component, close to the Coulomb energy called "relaxed" component. The relaxed component is present at all angles and for all particles. The quasi elastic component is present close to the grazing angle for atomic numbers close to that of the projectile. The relaxed cross section

---

*Work done under the auspices of the Energy Research and Development Administration.

†On leave from Institut de Physique Nucléaire, Orsay, France.

‡Sloan fellow 1974-76.

¶On leave from DphN/MF-CEN Saclay, France.

increases with atomic number for Z > 9. The increase in cross section is sharper for the lower bombarding energy. The angular distributions are forward peaked, in excess of $1/\sin\theta$ for all the measured atomic numbers. The forward peaking is larger for particles close in Z to the projectile. The results are interpreted in terms of characteristic times associated with a short-lived intermediate complex. The cross sections and angular distributions are satisfactorily reproduced on the basis of a model accounting for a diffusion process occurring along the mass asymmetry coordinate of the intermediate complex.

Nuclear Reactions: $^{40}Ar + ^{107,109}Ag$; E_{Ar} = 288 Mev, 340 Mev. The emitted fragments have been identified up to Z = 30. For each Z the kinetic energy distribution, the cross section and the angular distribution have been measured.

* * * * * * * * * * *

1. Introduction

Traditionally nuclear reactions have been classified into two well defined categories: the direct reactions and the compound nucleus reactions. In the first class of reactions, one or very few degrees of freedom of the target and of the projectile nucleus are involved, on a time scale of the order of one nuclear period ($\sim 10^{-22}$ sec). The trademarks of such reactions are a small degree of inelasticity, as determined from the kinetic energies of the products, and a strong peaking of the angular distributions in the general region of the grazing angle. On the other hand, compound nuclear reactions are characterized by the involvement of many nuclear degrees of freedom on a time scale strongly dependent upon excitation energy, but usually orders of magnitude larger than one nuclear period. The kinetic energy distributions of the compound nucleus

decay products show that the reaction occurs with an extreme degree of inelasticity. Furthermore, the center of mass angular distributions of the emitted particles are symmetric about 90°.

These two situations, so well represented experimentally, are by no means unique. Rather they ought to be considered as extreme cases of a continuous process of relaxation, whereby the reacting system evolves in time from the entrance channel into more and more complex dynamical configurations leading eventually to the fully randomized compound nucleus structure. Evidence of intermediate situations has been observed from time to time with ordinary light projectiles. Doorway states, giant resonances and pre-equilibrium particle emission are examples, now fairly common, of this state of affairs.

Heavy ion reactions seem particularly suitable for the study of a new class of intermediate phenomena associated with the relaxation process leading from entrance channel to compound nucleus. The reason for this expectation is based upon the substantial excitation of collective modes which must inevitably occur as two distinct large nuclei tend to melt into a single, near spherical, compound nucleus. Furthermore, the large excitation energies, frequently involved in such reactions, would lead to extremely short compound nucleus decay times, dangerously close to the characteristic vibrational and single particle periods. Also, the large angular momenta involved in such reactions drastically reduce or completely eliminate the fission barrier, thus compromising the stability of the hypothetical compound nucleus towards collective deformation.

This situation appears to be extremely favorable for the study of the relaxation processes associated with various collective degrees of

freedom. A number of studies with heavy ion reactions show indeed that this is the case.[1-11] The patterns of the kinetic energy distribution associated with the reaction products show that frictional and viscous phenomena are at work. The initial kinetic energy is dissipated as the system moves through an intermediate "quasi elastic" stage and eventually reaches a final completely "relaxed" state. The mass/charge distributions also show a lack of equilibration, especially visible in Kr induced reactions on heavy targets.[9-11] The angular distributions, substantially different from those expected for a compound nucleus, also indicate a diffusive evolution of the mass/charge asymmetry degree of freedom as a function of time.[12,13]

In the present paper the reaction induced by ^{40}Ar on a natural Ag target has been studied at two different bombarding energies: 288 Mev and 340 Mev. The atomic numbers of the fragments have been identified at certain angles as far as $Z \sim 30$, close to the symmetric splitting. The kinetic energy spectra, the cross sections and the angular distributions for each individual atomic number have been measured at both bombarding energies. Special attention has been given to the measurement of angular distributions. A theoretical model, involving diffusion along the mass asymmetry coordinate of a thermalized intermediate complex, has been developed and used in order to predict both cross sections and angular distributing as a function of atomic number.[12,13] The agreement between experiment and theory is excellent, thus giving confidence that relaxation times can be determined for various collective degrees of freedom.

2. Experimental techniques

The 288 Mev and 340 Mev Ar beams were provided by the Berkeley Super-Hilac. Most commonly, the 750 KV injector EVE was used, although, at

times, the 3 MV injector ADAM was employed. The beam was collimated to a spot approximately 3 mm. in diameter on the target. A Faraday cup was used to collect the beam that had crossed the target, and the current from the cup was monitored and integrated by means of a standard electrometer. The targets employed in the experiment were self-supported natural Ag foils, obtained by evaporation. This target thickness (~300 $\mu g/cm^2$) was such that no appreciable degradation of the beam energy nor of the emitted particle energies occurred.

The products of the reactions were detected and identified by means of two ΔE, E telescopes mounted on two independent arms rotating around the center of the scattering chamber. The ΔE counters were gas counters. In the early stage of the experiment, a ΔE gas proportional counter was used.[14] This detector, operated with a mixture of Ar, CH_4 (90%, 10% in volume respectively) at ~ 6 cm Hg pressure, provided atomic number resolution up to Z ~ 18. In the latter stages of the experiment, an ionization chamber of our own design was used.[15] This detector was operated both with the above mixture of Ar/CH_4 and with pure CH_4. The latter choice appears to be better both in terms of Z resolution (up to $Z \simeq 30$) and of signal rise-time. The gas pressure was stabilized by means of a Cartesian manostat. Pressures ranging from 6.0 to 8.0 cm Hg were used. A 50 µg plastic window (Formwar or VYNS) was used to separate the counter from the vacuum of the scattering chamber. The entrance window of the counter was located at 6 cm. from the target center and the solid angle, defined by the window, was typically $2.0\ 10^{-3}$ sr. The E detectors were Si solid state counters, 300 µm thick.

A schematic diagram of the electronic equipment is shown in fig. (1).

The pulses coming from the two telescopes were fed to a standard linear and logic circuitry and were routed to a single ADC system through an analog multiplexer. The digitized information, as well as the necessary identification markers, were fed to a PDP 15 computer event by event through a CAMAC system. The data, properly packaged, were then recorded on a magnetic tape. On-line monitoring was performed by means of an x, y storage scope.

The data were analyzed off-line on a PDP9 computer and, during the experiment, two dimensional ΔE-E maps were printed to check the performance of the system in greater detail.

3. Data reduction

a). The Z identification.

The printed ΔE-E maps show well defined valleys separating one element from the other. When using a ΔE ionization chamber, the peak to valley ratio is > 10 for Z ~ 10 and it decreases to ~ 3.0 around Z = 20 and to ~ 1.5 around Z = 30 (fig. 2). The absolute identification of the atomic number of any fragment can be made if just one atomic number is determined. In the forward angles, the elastically scattered beam(Z=18) makes itself quite visible. In the backward direction one can always rely upon the identification of Z = 9 from its unusually low cross section and of Z = 6 from its very high cross section. In this way it was always possible to identify the various Z's even prior to the energy calibration on the E and ΔE detectors. Each valley between Z's was identified by connecting a few points in the ΔE-E map. The coordinates of these points together with the Z identification, were fed to a PDP9 computer on punched cards for the evaluation of the kinetic energy distributions and of the cross

sections associated with each atomic number.

b). Energy calibration and Kinetic energy spectra.

The most accurate energy calibration was obtained by means of the elastically scattered beam. The energy deposited in the ΔE counter was computed from the Northcliff and Schilling tables and from the thickness and nature of the gas in the ionization chamber. The energy deposited was typically a few MeV. In order to calibrate the ΔE counter it was assumed that all of the charges created into the gas were collected. This is not quite true both at the entrance and at the exit of the counter, due to the weaker electric field. This may introduce an uncertainty of $\sim$ 5% in the absolute value of the ΔE energy. A 3% additional uncertainty should be considered because the pressure of the gas was not measured inside the detector but slightly upstream. The relative uncertainty of the total energy may become serious for large Z' at backward angles, because these fragments deposit a larger fraction of their energy into the ΔE counter. The energy deposit in the E counter was obtained by difference, taking into account the energy loss in the pastic window. No pulse height defect was assumed in the energy calibration.

c). Dead layer correction.

Corrections to the measured kinetic energies of the particles were made for the energy losses which occur both within the target and in the plastic window. The target correction was made by assuming that all the fragments originated in the middle layer of the target. For each atomic number, a 5th degree polynominal fit to the Northcliff and Schilling table was used to calculate the energy loss. This correction is important for

the higher atomic numbers at the lowest laboratory energy. In the worst cases, the correction may be as large as 10 - 20% of the measured energy. However, in most of the cases the corrections were smaller than 5% of the measured values.

4. Transformation from laboratory to center of mass systems.

The transformation from laboratory to center of mass system was performed on the doubly differential cross section $\left.\frac{\partial^2\sigma}{\partial\Omega\partial E}\right|_{lab}$. For each fragment and for each angle θ_{lab}, the corresponding θ_{cm} & $\left.\frac{\partial^2\sigma}{\partial\Omega\partial E}\right|_{cm}$ were computed. At the same time the integrated cross section $\left.\frac{\partial\sigma}{\partial\Omega}\right|_{cm}$, the mean center of mass energy $\bar{E}_{cm} = \left(\left.\frac{\partial\sigma}{\partial\Omega}\right|_{cm}\right)^{-1} \sum E_{cm} \left.\frac{\partial^2\sigma}{\partial\Omega\partial E}\right|_{cm}$ and the mean center of mass angle $\bar{\theta}_{cm} = \left(\left.\frac{\partial\sigma}{\partial\Omega}\right|_{cm}\right)^{-1} \sum \theta_{cm} \left.\frac{\partial^2\sigma}{\partial\Omega\partial E}\right|_{cm}$ were also computed. In order to perform the transformation to the center of mass system, an assumption must be made about the masses A_1, A_2 of the fragments which are not measured in this experiment. Two assumptions have been made. The first is:

$$A_1 = 2Z_1;$$

the second is:

$$A_1 = (A_1 + A_2)\, Z_1/(Z_1 + Z_2);\ A_1 + A_2 = 148$$

The differences in the resulting center of mass kinetic energies and cross sections are of the order of 2 - 3%. The distribution in θ_{cm} for a given θ_{lab} due to the laboratory kinetic energy distribution is

particularly important around 90°. The FWHM in angle can be here as large as 5° to 10°. In principle one needs to know the angular distribution in the center of mass in order to obtain the correct center of mass kinetic energy distributions and cross sections. However, due to the small spread in angle, and to the fact that the correction terms to the integrated cross section arise only from the second derivative of the angular distribution with respect to angle, the errors introduced by neglecting such correction should not be larger than 2 - 3%.

5. Presentation of the experimental data and discussion

a) The kinetic energies

Two distinct components are observed in the kinetic energy spectra, similar to those observed in other heavy ion reactions.

The first component, which we call "quasi-elastic component" because its energy is strongly related to that of the projectile, is observed at angles close to the grazing angle and for atomic numbers close to that of the projectile. The energy distribution of this component is very broad and its most probable value decreases as one moves further away from the projectile. Examples of quasi-elastic components can be seen in the spectra shown in fig. (3). The origin of this component appears to be related to the initial stages of dissipation of kinetic energy associated with large l wave entrance channels.

The second component, to which this work is particularly addressed, is called the "relaxed component". Such component is observed at all angles and for all particles. It is characterized by a lower energy than the "quasi-elastic" component and appears to increase weakly with the bombarding energy. The relaxed components are approximately gaussian-

shaped and several examples can be seen in fig. (3).

The most probable relaxed kinetic energies in the laboratory system are shown in fig. (4) for the 288 MeV bombarding energy. The great spread of these values as a function of angle is mainly kinematic in nature. A similar spread of values is observed for the 340 MeV bombarding energy. After transformation to the center of mass, the most probable kinetic energy for each fragment seems to be rather insensitive to the angle of measurement (fig. 5). The systematic discrepancies that remain (somewhat larger energies at smaller angles) are rather small though they are particularly noticeable for Z's close to that of the projectile.

The dependence of the most probable center-of-mass energies upon atomic number is easily identified as that of the Coulomb energies of two touching fragments. The experimental values are somewhat lower than the Coulomb energies of two touching spheres, and are fairly close to the predictions for two touching spheroids allowed to attain their equilibrium deformation.

These calculations, shown in fig. (6), have been performed not with the idea of fitting the data, but in order to show the unmistakable trend, characteristic of the Coulomb energies, present in the data. A conclusion that can be drawn fairly safely from the association of the observed kinetic energies with the Coulomb energies is that only two main fragments are produced in the reaction. The binary splitting has been satisfactorily tested in coincidence experiments on the same system at the same bombarding energies. A comparison between the two bombarding energies shows that the kinetic energies of the fragments are about the same. There is a marginal evidence that the 340 MeV experiment

has slightly higher fragment kinetic energies; however the effect is well within the uncertainties of the experiment. The most probable energies and widths (FWHM) of the kinetic energy distributions averaged over angles are shown in fig. (6). The widths range between 20 and 30 MeV, the maximum widths being in the region of Z = 18. This, like the maximum in kinetic energies, has nothing to do with the fact that Z = 18 is the atomic number of the projectile. It is just accidental that the conservation of linear momentum (which decides the kinetic energy ratio of the two fragments), together with the Coulomb energy dependence upon Z, lead to a maximum in fragment kinetic energy around Z = 18. At 340 MeV the widths appear to be larger by ~ 5 MeV than at 288 MeV.

The overall features of the "relaxed" kinetic energy component of the cross section are similar to those of a compound nucleus reaction. In fact, they remind one of the fission process. The closeness of the kinetic energies to the Coulomb energies, their approximate independence from angle and, what is more important, from bombarding energies, suggests strongly that the entrance channel kinetic energy has been completely transferred into the internal degrees of freedom in from of heat. We have thus assigned the name "relaxed" to this kinetic energy component. It should be stressed that while the kinetic energies are consistent with the compound nucleus hypothesis,[7] they are no proof that a compound nucleus has been formed. The only conclusion that can be drawn is that, for each splitting configuration, no excess kinetic energy above that required by the thermal equilibrium seems to be observed.

b) The Z distribution

The laboratory differential cross sections $\left.\frac{d\sigma}{d\Omega}\right|_{lab}$ as a function of atomic number are shown for different laboratory angles in fig. (7). These cross sections have been obtained by integration over the relaxed peaks

of the kinetic energy distributions. Whenever the relaxed and the quasi-elastic peaks could not be separated, the cross sections have not been recorded. The center of mass cross sections are plotted for each Z as a function of angle in fig. (8).

The center of mass cross sections integrated over the experimental angular range, and extrapolated to a fixed angular range (30° to 130°) are given in Table I.

The first observation to be made concerns the great variety of products formed in the reaction. Fragments of all atomic numbers up to the symmetric splitting are produced with cross sections ranging within a factor of 10 at 288 MeV bombarding energy and within a factor of 5 at 340 MeV bombarding energy. The cross sections appear to fluctuate strongly, with a possible slight decreasing trend, from Z = 6 to Z = 9 where a deep minimum is observed. From Z = 9 to Z = 18, the cross sections rise rapidly and above Z = 18 they appear to level out. Superimposed upon the general trend, a remarkable even-odd alternation is visible, expecially for lower atomic numbers. The reason why even atomic numbers are favored with respect to odd atomic numbers is not completely clear. It has been observed for many different heavy ion reactions,[3,6,7] so that it does not seem to depend strongly on the entrance channel. In fact, it is possible that the effect may be due to secondary particle evaporation from the main fragments. Especially interesting in this regard is the Z = 9 fragment which has the lowest cross section. It is possible that this fragment, produced with substantial excitation energy, easily loses the loosely bound odd proton. The data, taken at two different bombarding energies, show that the cross sections are increasing more rapidly with Z at the lower bombarding energy. A glance to fig. (8) where the angular distributions are shown, indicates that, for high Z's the cross sections are about the same at

both bombarding energies while at low Z's the cross sections are higher for the higher bombarding energy. This last feature can be understood in terms of a simple statistical argument. In the limiting case of compound nucleus decay, the fragment yield Y(Z) should be approximately of the form:

$$Y(Z) \propto \exp(-V_Z/T)$$

where V_Z is the potential energy of the system formed with the two fragments in contact and T is the temperature. A typical set of curves for V_Z as a function of Z at various angular momenta is shown in fig. (9). The above equation shows that, as the temperature increases, the cross section, initially concentrated around the low potential energy regions, spreads out in such a way that the relative cross sections rise in the regions of large potential energies and decrease in the regions of low potential energy. Again this does not imply that a compound nucleus has been formed. Rather it shows that the reaction is very sensitive to the ratio V_Z/T.

c) The angular distributions

The center of mass angular distributions are shown in fig. (8). The plotted data have been checked in detail for the presence of quasi-elastic components. Even at the most forward angle, the contributions of quasi-elastic components are less than 3%. In other words, the angular distributions contain exclusively the "relaxed" component of the cross section.

The angular distributions are substantially forward peaked, quite in excess of $1/\sin\theta$, more sharply peaked close to Z = 18 than for lower atomic numbers. No evidence of backward peaking is present other than a flattening occurring at about 120°. Apart from the absolute value of

the cross sections, the shapes of the angular distributions are remarkably similar at both bombarding energies.

These angular distributions represent the first direct evidence that the compound nucleus hypothesis is not satisfied for the present reactions at least for a large fraction of the observed products. This is not surprising in view of the expected role of the collective modes as mentioned in the introduction. Furthermore one can make simple considerations associated with the energy and angular momentum of the system. In fig. (10) the compound nucleus decay time, approximated by the neutron decay time, is compared with the rotational and vibrational periods. It appears that already at 288 Mev bombarding energy the rotational period and the vibrational period are about the same as the compound nucleus lifetime, while the nucleonic period is less than one order of magnitude smaller. This simple calculation illustrates the fact that for the present reactions one should expect substantial evidence for incomplete equilibration, since the characteristic collective times become comparable with the decay times.

The lack of symmetry about 90° in the angular distributions indicates that the decay time is indeed shorter than the mean rotational period. Also, the fact that the kinetic energies associated with these cross sections are completely thermalized implies that the relaxation time associated with the transfer of the entrance channel kinetic energy into the internal degrees of freedom is shorter than the mean rotational period.

At this point, one may wonder about the mechanism involved in these processes. Perhaps the clearest hint is given by the change in angular distributions as a function of Z. We have already observed that the

angular distributions are more forward peaked in the vicinity of the projectile, and less forward peaked for fragments far removed from the projectile. This suggests that particles closer to the projectile are formed, and thus can be emitted, on a shorter time scale, while particles far removed from the projectile are formed and emitted on a larger time scale. Therefore a definite time evolution along the mass/charge asymmetry coordinate is visible. Such a time dependence, together with the thermalized kinetic energy is suggestive of a diffusion process taking place along the mass/charge asymmetry coordinate in a short lived intermediate complex.[12,13] This intermediate complex can be represented as composed of two fragments in contact. The intermediate complex is at high temperature (arising from the dissipated kinetic energy) and is rotating rapidly. As the complex rotates, it diffuses along the asymmetry coordinates and decays.

In a recent paper Moretto and Sventek proposed the following model.[13] After the collision between the target and the projectile, the kinetic energy is dissipated as the two fragments slide on top of each other until they eventually stick. A slippage in angle proportional to the initial tangential velocity of the projectile is assumed. As the intermediate complex rotates, diffusion along the mass asymmetry takes place. The diffusion process is described in terms of the master equation in which the statistical weights are evaluated from the potential energies and the temperatures of the intermediate complex. As the system rotates and diffuses, it decays exponentially in time. The cross sections and angular distributions are calculated by specifying the window in ℓ waves associated with this reaction process (the ℓ wave window can be estimated from the knowledge of the evaporation residue cross section and from the total

relaxed cross section). An example of this calculation applied to the system studied in this paper is shown in fig. (11). It can be observed that the cross sections and angular distributions are reproduced with remarkable accuracy.

The theory seems able to reproduce the forward peaking in the angular distributions, as well as the dependence of the forward peaking with Z.

While many aspects of the theory are quite crude and uncertain, it appears that an initial step has been made towards the understanding of the equilibration processes in general and towards the determination of nuclear relaxation lines in particular.

6. Summary and Conclusion.

The study of the reaction Ag + Ar has revealed the presence of a "relaxed" component which accounts for a large fraction of the total cross section. This component is observed over a great range of atomic numbers. The kinetic energy distributions are nearly independent of bombarding energy. Their most probably values correlate with the energies to be expected from Coulomb repulsion and their widths seem to be consistent with a statistical interpretation. From this evidence one is led to the conclusion that the kinetic energies are indeed thermalized or relaxed. The cross sections show a broad change/mass distribution which apparently is sensitive to V_z/T, although it is not possible to conclude from the experimental evidence whether these distributions are equilibrated. The angular distributions are forward peaked, more so for fragments closer in Z to the projectile. From this one can infer that both the decay times and the relaxation time for the thermalization of the kinetic

energy are shorter than the mean rotational period. The change in angular distribution with Z indicates that the mass symmetry degree of freedom equilibrates in a time comparable to the rotational period. The experimental data suggest that the latter equilibration process proceeds through a diffusion mechanism whereby nucleons are transferred between two fragments in contact and in thermal equilibrium. The study of angular distributions appears to be a most promising technique for the determination of relaxation times. In particular, the diffusion along the charge mass asymmetry coordinate can be studied quite nicely by investigating systems with various initial asymmetries in charge and or mass.

REFERENCES

1. J. Galin, D. Guerreau, M. Lefort, J. Péter and X. Tarrago, Nucl. Phys. A 159 (1970 461.

2. A. G. Artukh, V. V. Avdeichikov, G. F. Gridnev, V. L. Mikheev, V. V. Volkov and J. Wilczinski, Nucl. Phys. A167 (1971) 284.

3. L. G. Moretto, D. Heunemann, R. C. Jared, R. C. Gatti and S. G. Thompson, Physics and Chemistry of Fission 1973 International Atomic Energy Agency, Vienna, 1974 V. II p. 351.

4. A. G. Artukh, G. F. Gridnev, V. L. Mikheev, V. V. Volkov and J. Wilczinski, Nucl. Phys. A211 (1973) 299.

5. A. G. Artukh, G. F. Gridnev, V. L. Mikheev, V. V. Volkov and J. Wilczinski, Nucl. Phys. A215 (1973) 91.

6. S. G. Thompson, L. G. Moretto, R. C. Jared, R. P. Babinet, J. Galin, M, M. Fowler, R. C. Gatti and J. B. Hunter, Nobel Symposium on Superheavy Elements (1974). Physica Scripta Vol. 10-A.

7. L. G. Moretto, S. S. Kataria, R. C. Jared, R. Schmitt and S. G. Thompson, Lawrence Berkeley Laboratory Report LBL 4063, May 1975

8. For a complete list of references see A. Fleury and J. M. Alexander, Ann. Rev. Nucl. Sci. 1632-4 (1974) 279.

9. F. Hanappe, C. Ngô, J. Péter, B. Tamain, Physics and Chemistry of Fission 1973 International Atomic Energy Agency Vienna, 1974 V.II, p. 289.

10. F. Hanappe, M. Lefort, C. Ngô, J. Péter and B. Tamain, Phys. Rev. Lett. 32(1974) 738.

11. K. L. Wolf, J. P. Unik, J. R. Huizenga, V. E. Viola, J. Birkelund and H. Freiesleben, Phys. Rev. Lett. 33 (1974) 1105.

12. L. G. Moretto, R. P. Babinet, J. Galin and S. G. Thompson, Lawrence Berkeley Laboratory Report LBL 3444, November 1974.

13. L. G. Moretto and J. S. Sventek, Lawrence Berkeley Laboratory Report LBL-3443, November 1974.

14. K. D. Hildenbrand, H. H. Gutbrod, W. V. Oertzen and R. Bock, Nucl. Phys. A157 (1970) 297.

15. M. M. Fowler and R. C. Jared, Nucl. Inst. Meth. 124 (1975) 341.

TABLE I.

	E = 288 MeV				E = 340 MeV			
Z	$\theta^{c.m.}_{min}$ deg	$\theta^{c.m.}_{max}$ deg	$\int_{\theta_{min}}^{\theta_{max}} 2\pi\sin\theta\frac{d\sigma}{d\Omega}\,d\theta$ mb	$\int_{30^\circ}^{130^\circ} 2\pi\sin\theta\frac{d\sigma}{d\Omega}d\theta$ mb	$\theta^{c.m.}_{min}$ deg	$\theta^{c.m.}_{max}$ deg	$\int_{\theta_{min}}^{\theta_{max}} 2\pi\sin\theta\frac{d\sigma}{d\Omega}d\theta$ mb	$\int_{30^\circ}^{130^\circ} 2\pi\sin\theta\frac{d\sigma}{d\Omega}d\theta$ mb
7	28	141	3.9	3.5	36	134	6.9	7.4
8	26	143	5.2	4.5	35	135	7.9	8.1
9	28	141	3.0	2.7	36	135	5.2	5.5
10	28	140	5.6	5.1	36	135	7.9	8.6
11	24	140	7.1	5.9	30	135	9.1	8.1
12	23	138	11.7	9.9	37	134	11.1	11.9
13	26	141	12.8	10.9	32	134	13.2	13.0
14	26	141	17.5	15.2	33	125	17.1	18.3
15	22	123	19.3	17.2	32	115	14.5	15.9
16	42	94	9.3	15.9	32	120	18.3	19.0
17	37	104	12.4	18.9	45	109	11.5	21.3
18	—	—	—	—	—	—	—	—
19	—	—	—	—	45	114	15.3	24.5
20	—	—	—	—	39	106	16.0	24.4
21	—	—	—	—	39	107	16.8	25.2

Integrated center-of-mass cross sections for individual atomic numbers. The first cross section column gives the cross section integrated over the experimental angular interval. The second cross section column gives the integrated cross section over a fixed angular interval. Due to the interpolations and extrapolations used in the evaluation of the integrals, and to the other experimental uncertainties, the quoted values may be in error by about 20%.

FIGURE CAPTIONS

Fig. 1 Schematic diagram of the data collection system.

Fig. 2 Typical ΔE, E map obtained with a ΔE gas ionization chamber telescope. The contour lines show a good Z separation up and above Z = 30.

Fig. 3 Examples of center-of-mass kinetic energy distribution for various fragments, at various angles, and at both bombarding energies. In the distributions at 288 MeV bombarding energy, quasi elastic components of increasing intensities are seen close to the grazing angle, for Z = 15, 16, 17. The relaxed peaks of the kinetic energy distributions are seen to be nearly independent of angle. The distributions have been arbitrarily normalized to one another.

Fig. 4 Most probable kinetic energies in the lab system as a function of Z at various angles at 288 MeV bombarding energy.

Fig. 5 Most probable center-of-mass kinetic energies as a function of Z at various angles and at both bombarding energies.

Fig. 6 Center-of-mass most probable kinetic energies and widths (F.W.H.M.) averaged over angles, as a function of Z, at both bombarding energies. Only the relaxed components have been averaged. Missing error bars indicate that data were avaialble at a single lab angle. The upper curve corresponds to the

(Continued)

Fig. 6 kinetic energy expected from the Coulomb repulsion of two touching spheres: $E_{z_1} = \frac{A_2}{A_1 + A_2} 1.442 \frac{Z_1 Z_2}{r_o(A_1^{1/3} + A_2^{1/3}) +}$ MeV

(r_0 = 1.225 fm). The lower curve corresponds to the kinetic energy expected from the Coulomb repulsions of two liquid drop spheriods allowed to attain their equilibrium deformation.

Fig. 7 Lab, differential cross sections as a function of Z, for the various angles, at both bombarding energies.

Fig. 8 Center-of-mass angular distributions for the various Z's at both bombarding energies. The dashed line at Z = 21 corresponds to a 1/sin Θ distribution.

Fig. 9 Total potential energies of two touching spheres, measured with respect to the rotating spherical ground state of the combined system as a function of the Z of one of the two fragments. The potential energies are given for three values of the angular momentum.

Fig. 10 Characteristic collective times and compound nucleus neutron decay times (τ_n) as a function of bombarding energy and angular momentum. The angular momentum scale is such that, for a given bombarding energy it gives the RMS angular momentum of the combined system. The values of τ have been calculated both for a spherical compound nucleus (CN) and for a configuration of spherical target and projectile in contact (symbolized by a small circle touching a large circle).

Fig. 11 Experimental angular distributions and theoretical calculations on the basis of a diffusion model.[13]

Data Collection System

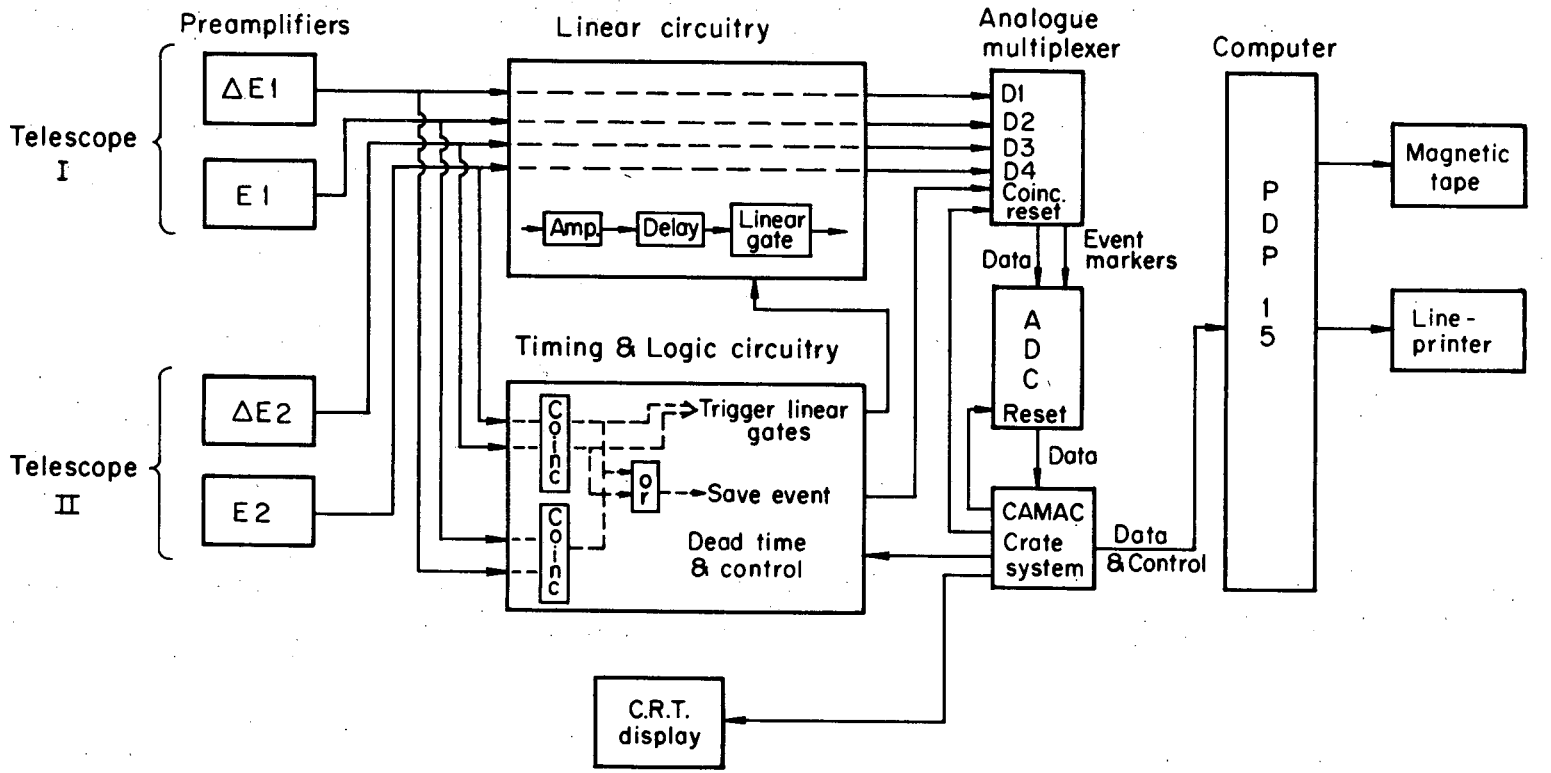

Fig. 1

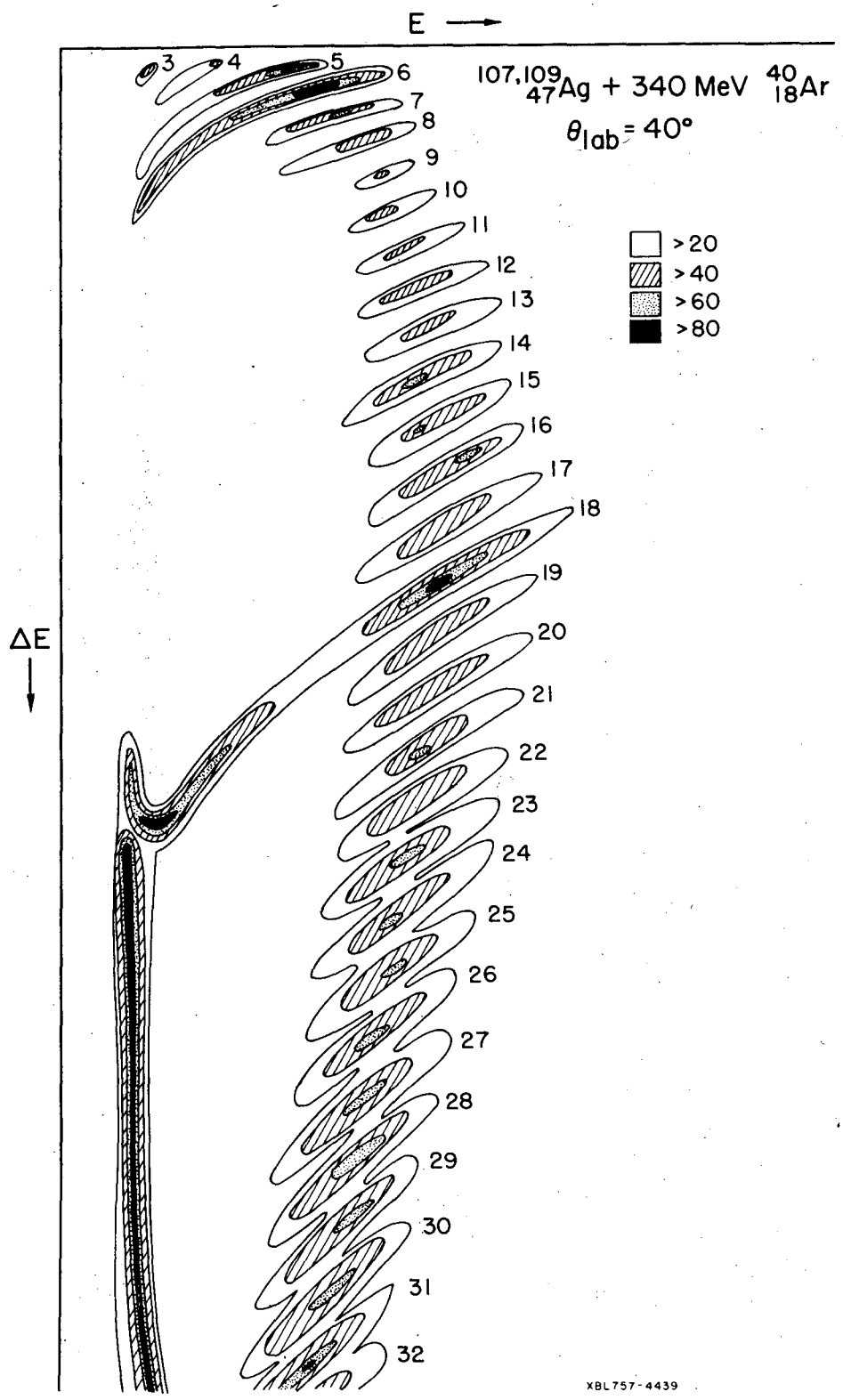
E
ΔE
107,109 47Ag + 340 MeV 40 18Ar
θlab = 40°
>20
>40
>60
>80
3
4
5
6
7
8
9
10
11
12
13
14
15
16
17
18
19
20
21
22
23
24
25
26
27
28
29
30
31
32
XBL757-4439

Fig. 2

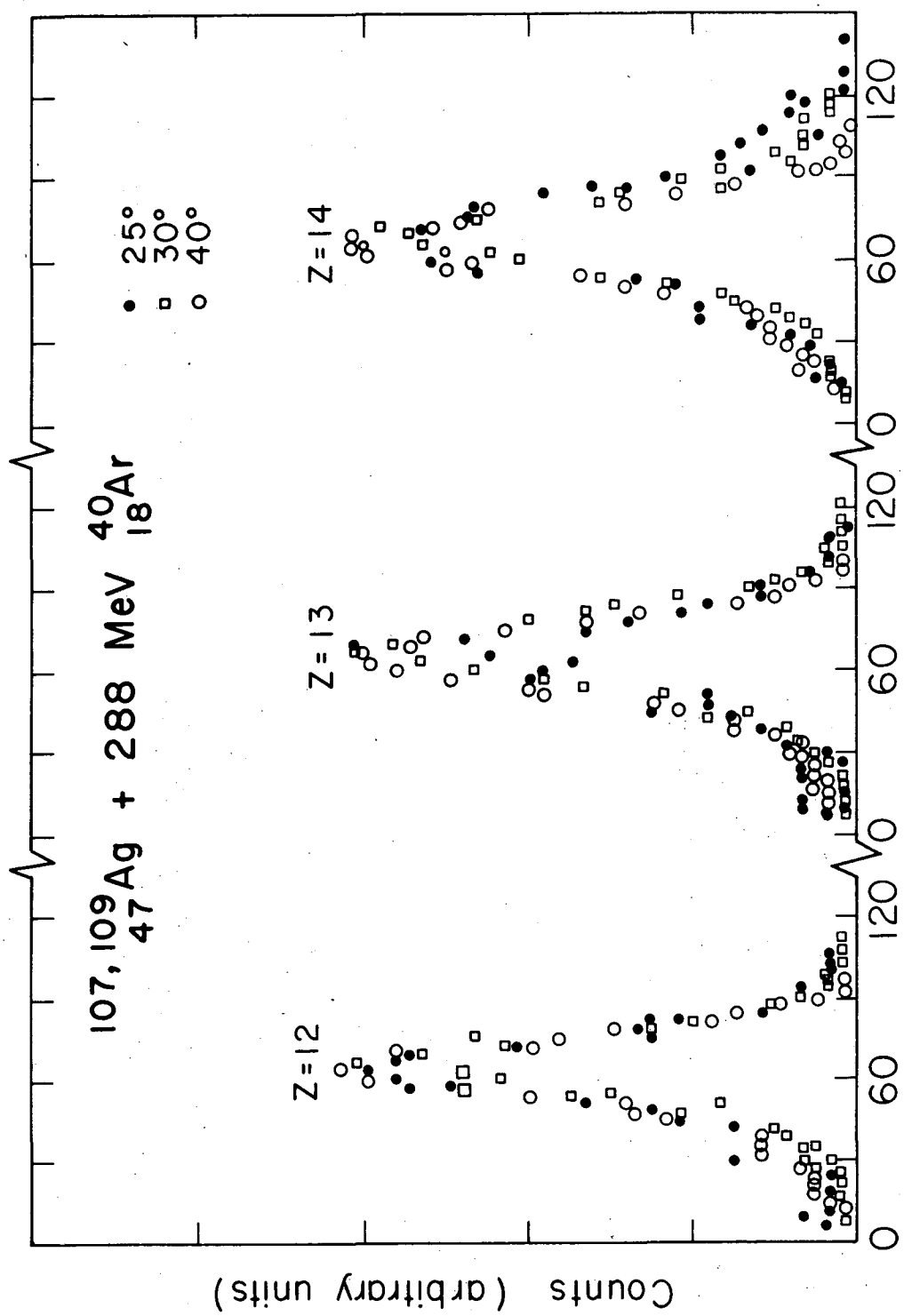

XBL756-3312

Fig. 3a

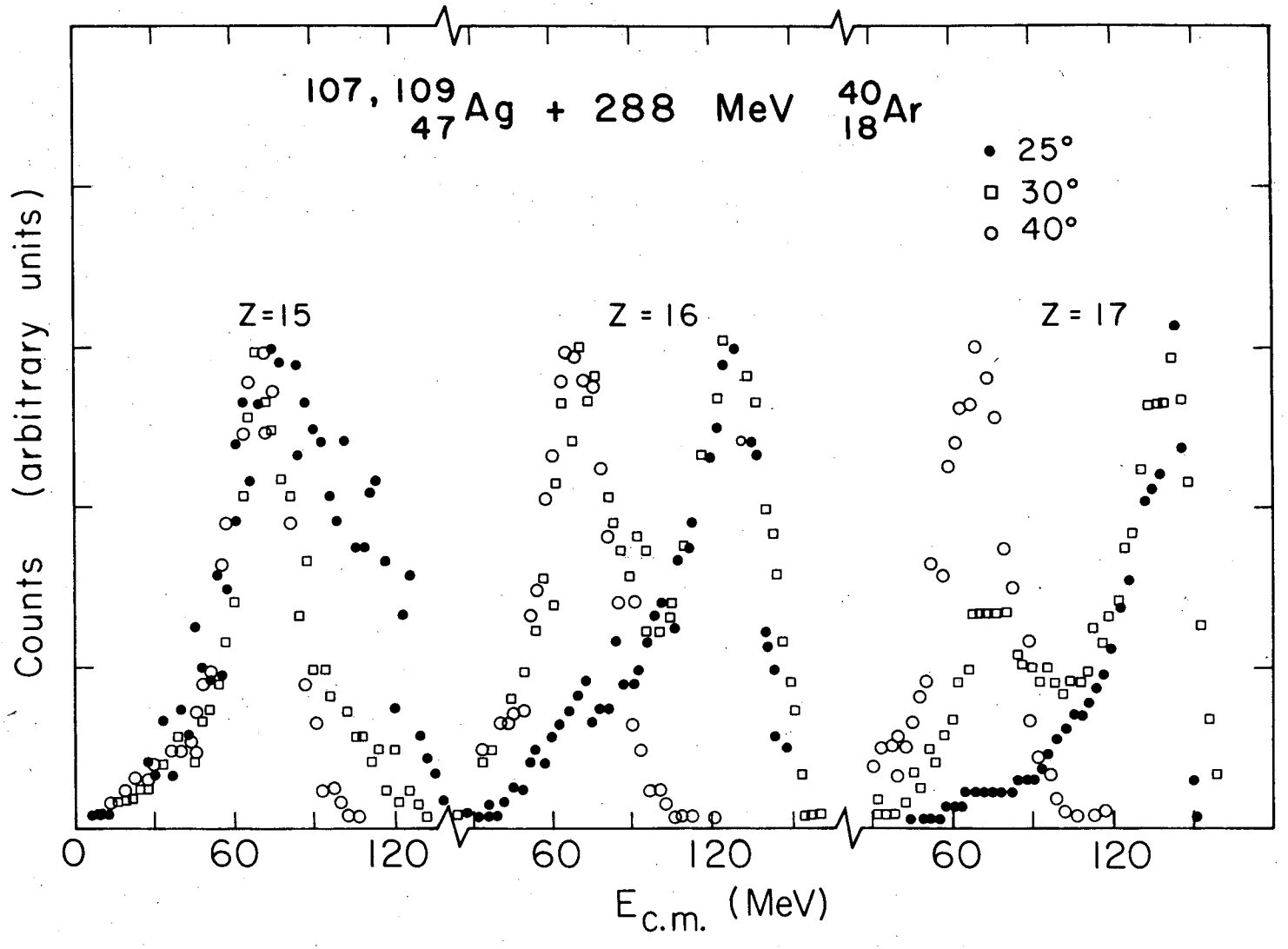

XBL756-3311

Fig. 3b

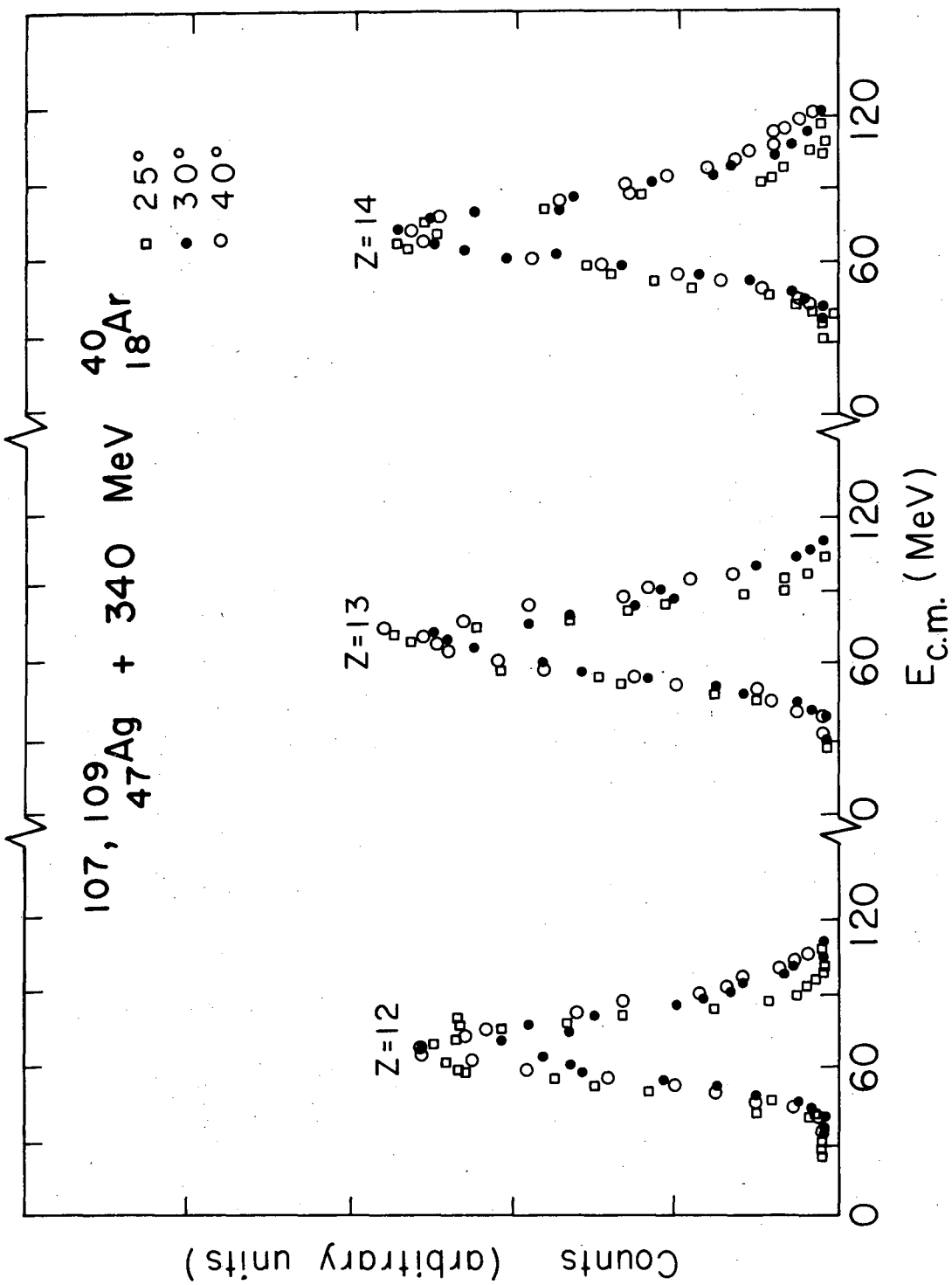

XBL756-3313

Fig. 3c

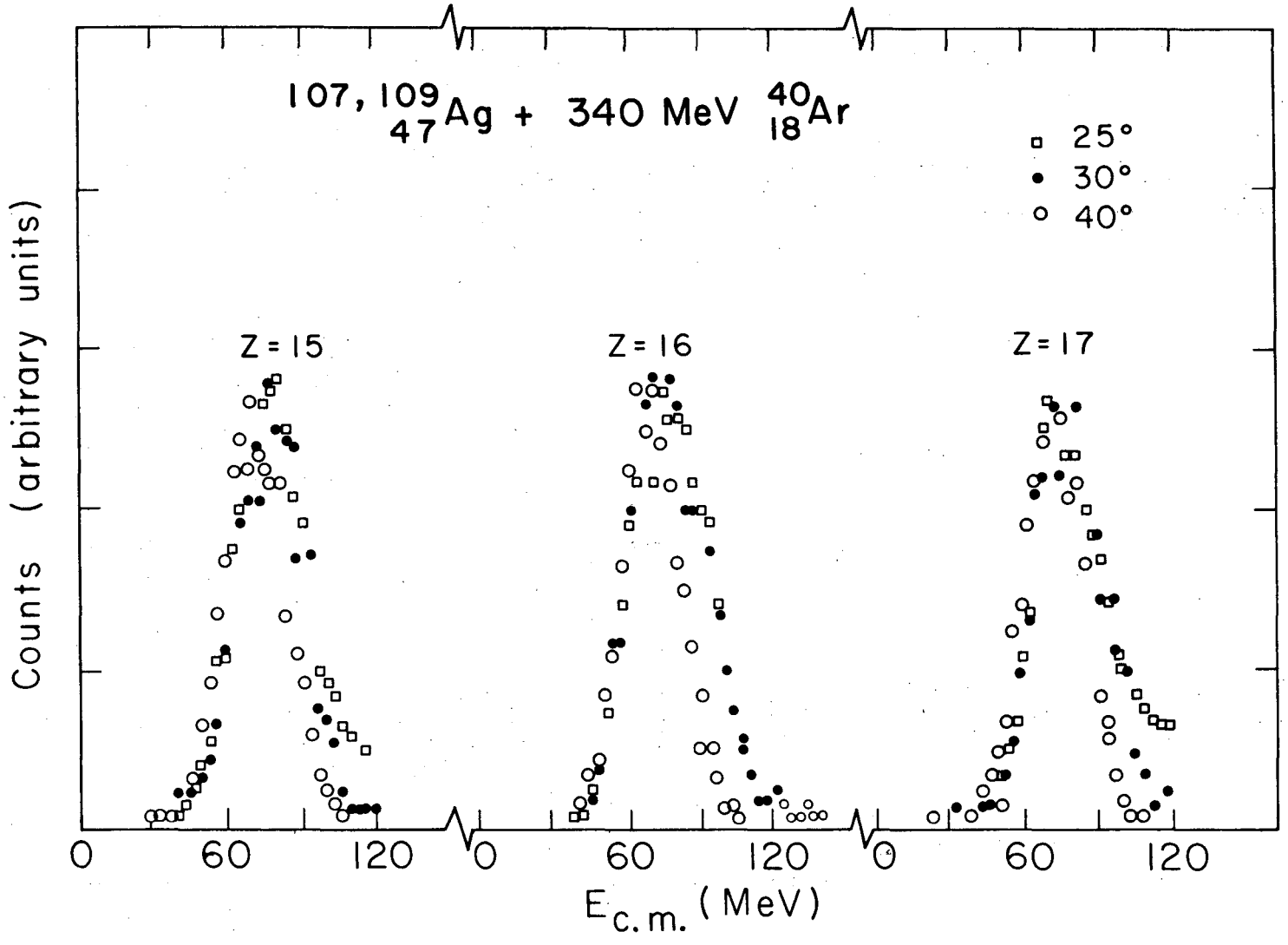

XBL756-3314

Fig. 3d

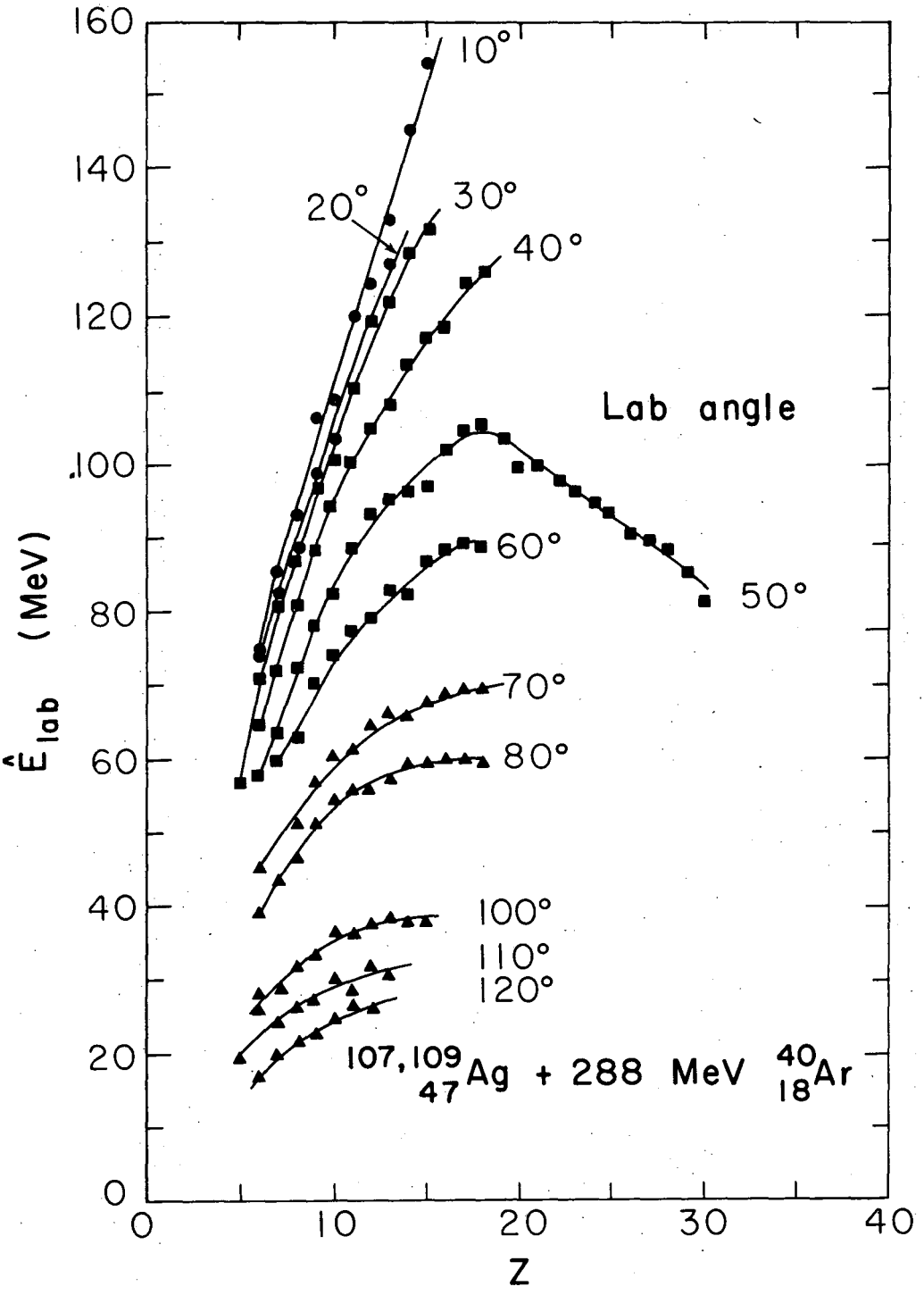
160
140
120
100
80
60
40
20
0
0
10
20
30
40
Z
$\hat{E}_{lab}$ (MeV)
10°
20°
30°
40°
Lab angle
50°
60°
70°
80°
100°
110°
120°
$^{107,109}_{47}Ag$ + 288 MeV $^{40}_{18}Ar$
XBL756-3309

Fig. 4

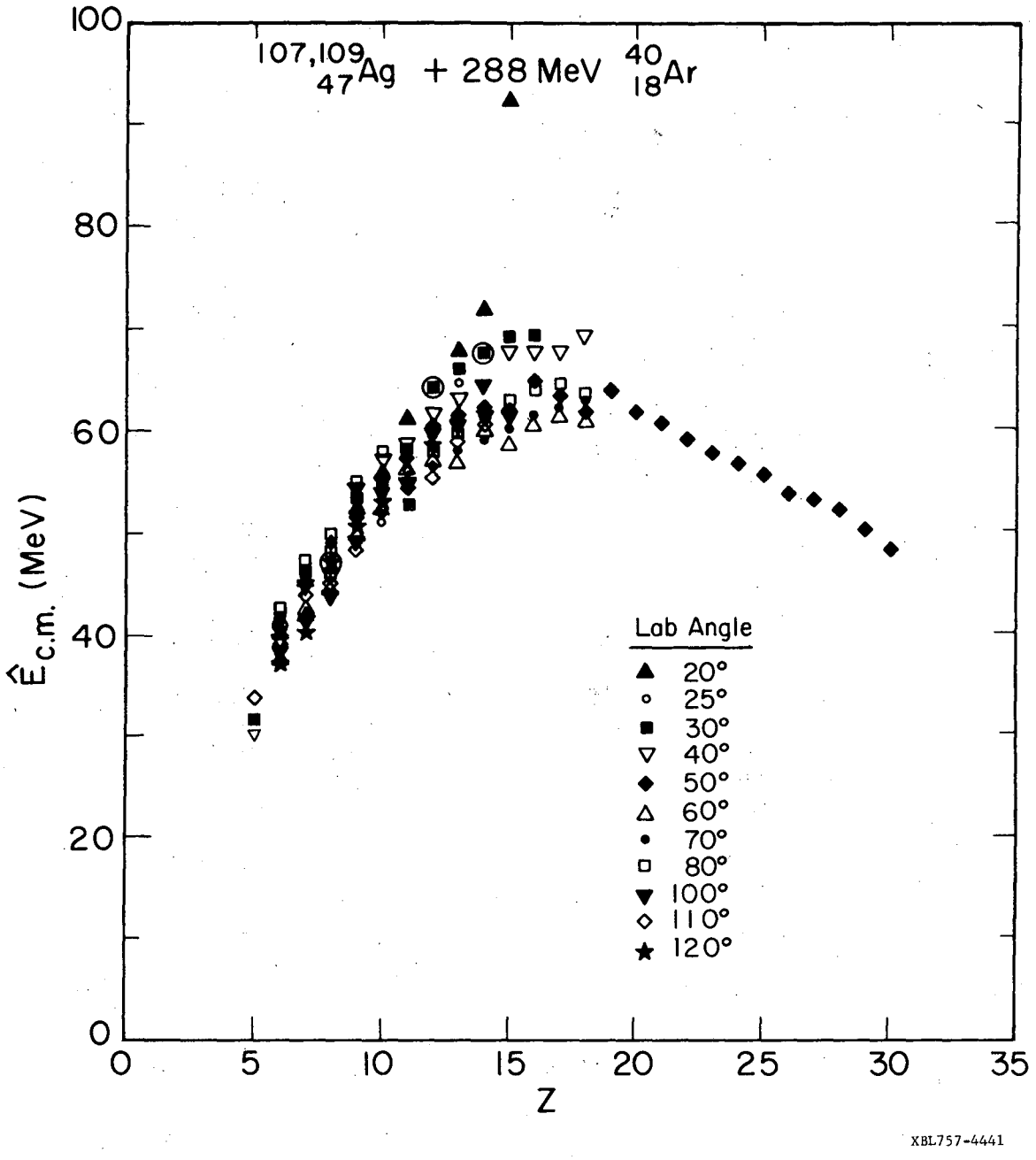
107,109 Ag + 288 MeV 40 Ar
47 18
Ê c.m. (MeV)
Z
Lab Angle
20°
25°
30°
40°
50°
60°
70°
80°
100°
110°
120°
0
20
40
60
80
100
0
5
10
15
20
25
30
35
XBL757-4441

Fig. 5a

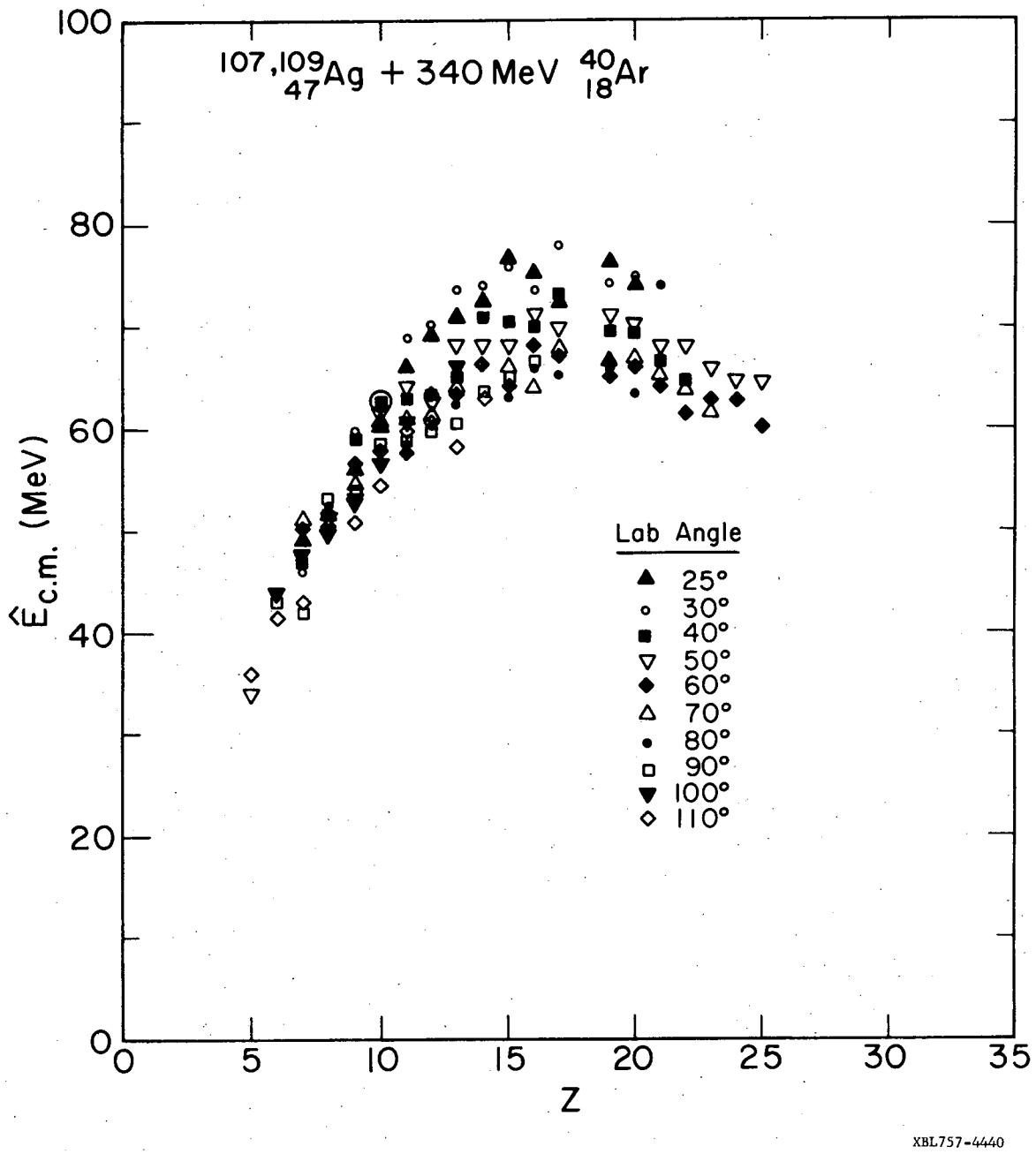
$^{107,109}_{47}Ag + 340\ MeV\ ^{40}_{18}Ar$
$\hat{E}_{c.m.}$ (MeV)
Z
Lab Angle
25°
30°
40°
50°
60°
70°
80°
90°
100°
110°
0
20
40
60
80
100
0
5
10
15
20
25
30
35
XBL757-4440

Fig. 5b

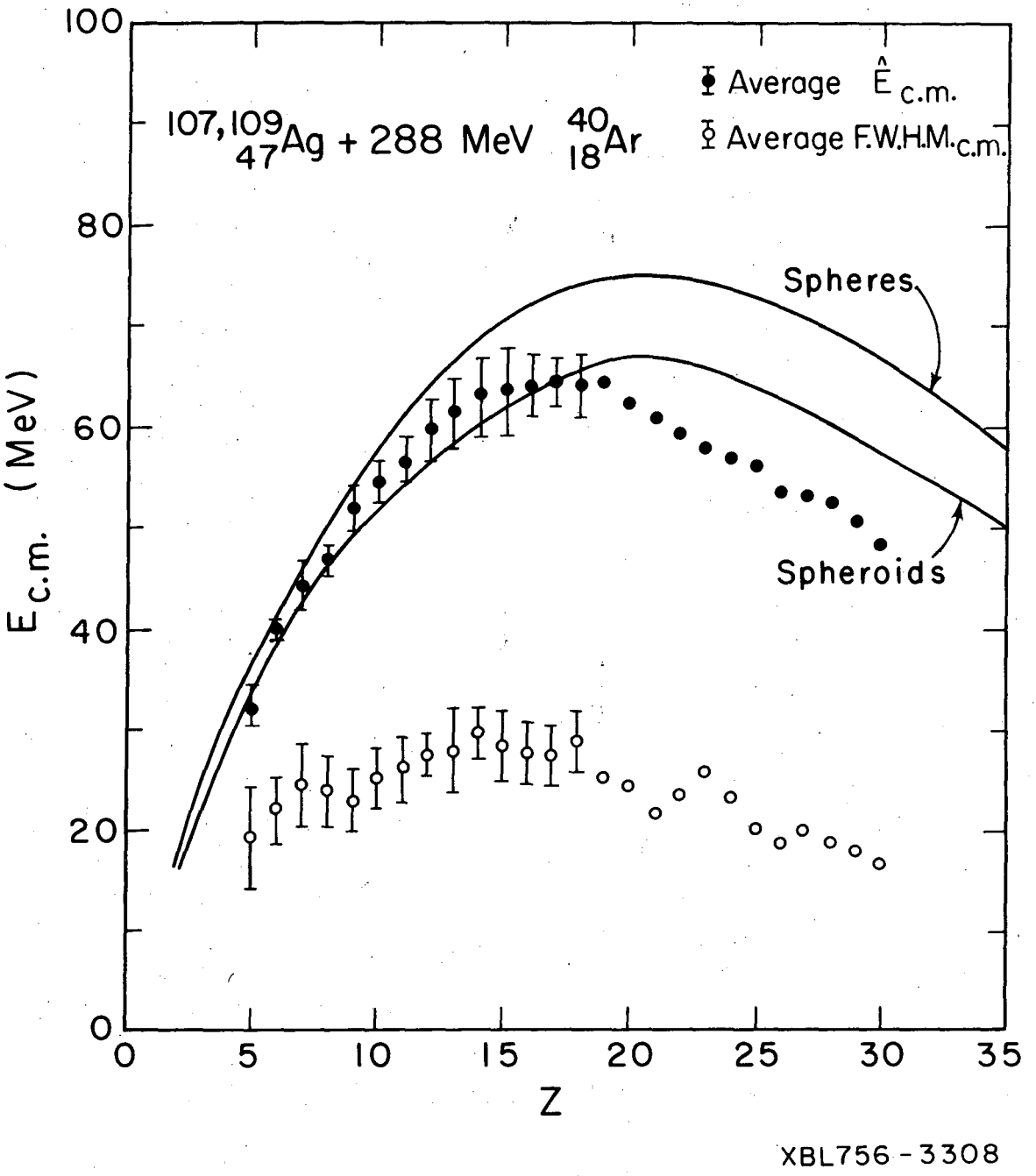

Fig. 6a

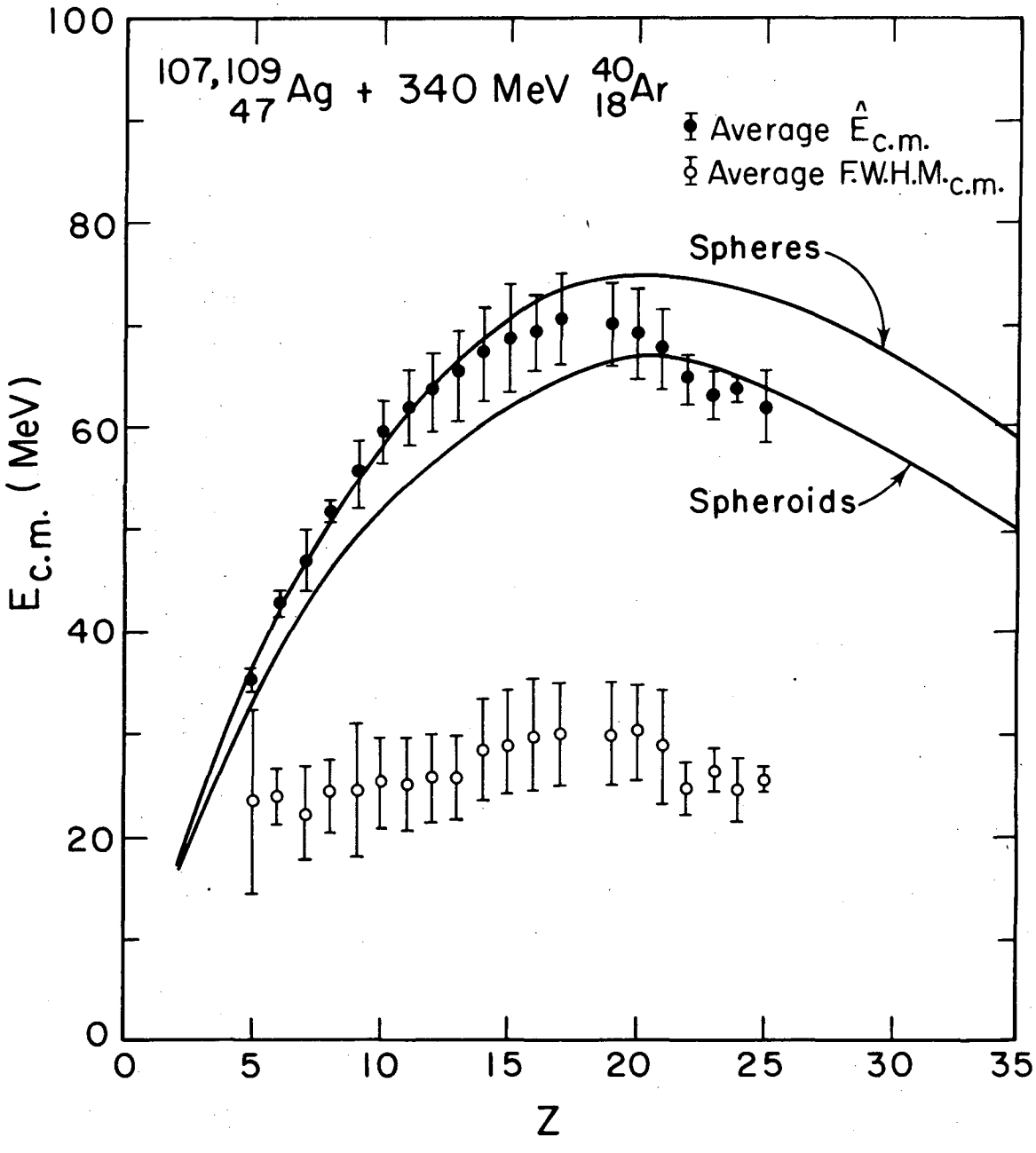

XBL756-3310

Fig. 6b

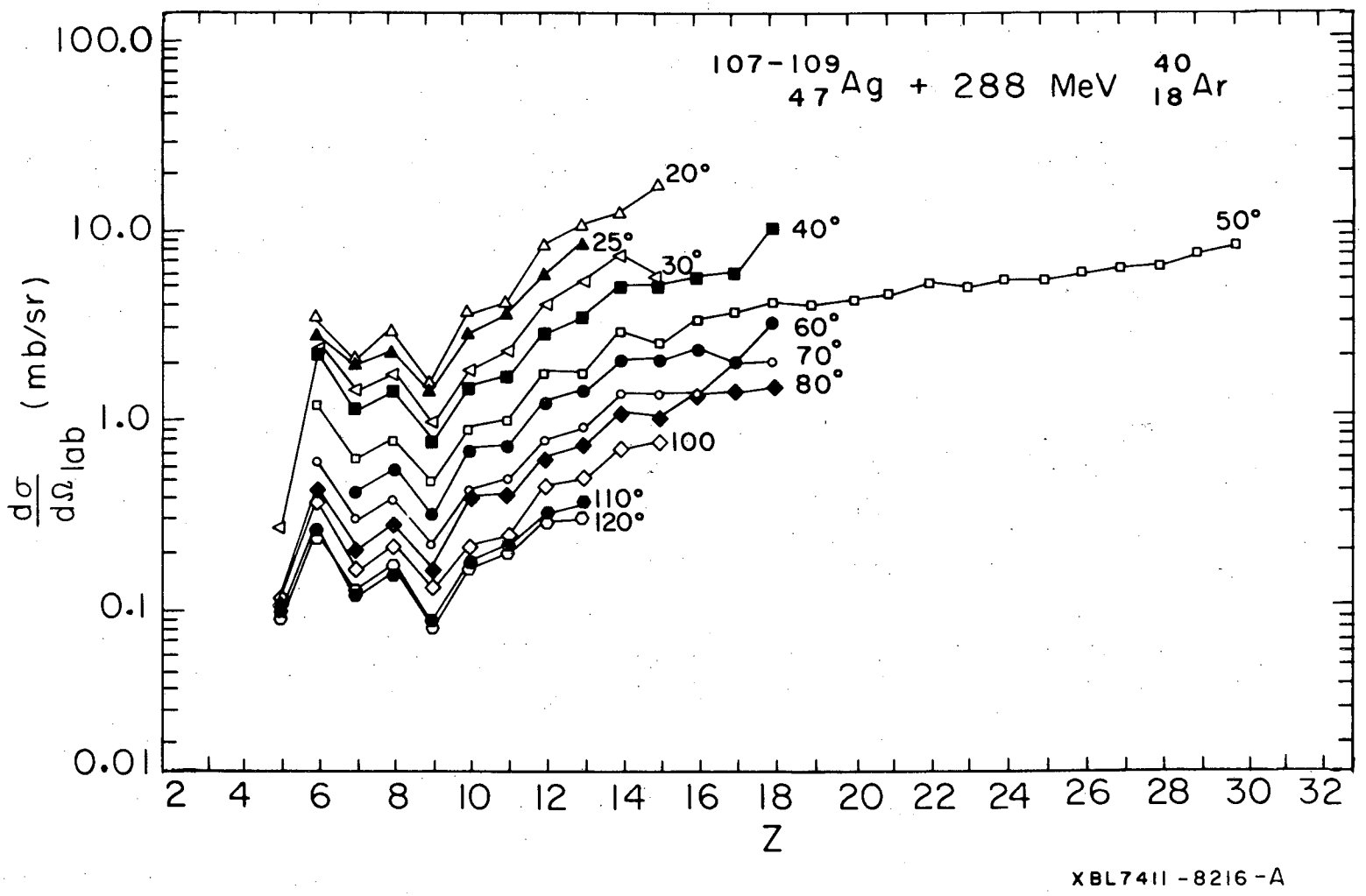

Fig. 7a

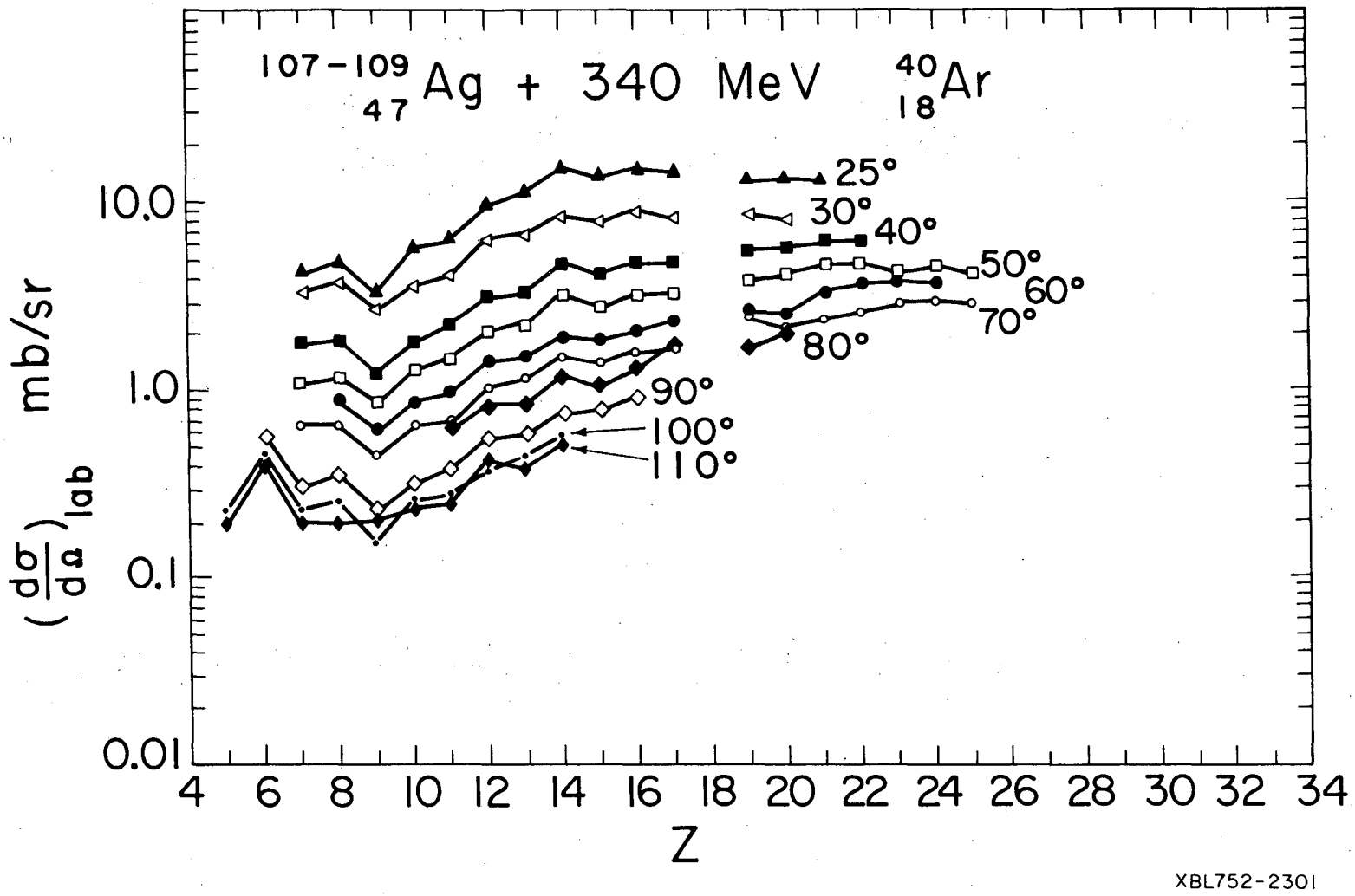
107-109 47 Ag + 340 MeV 40 18 Ar
25°
30°
40°
50°
60°
70°
80°
90°
100°
110°
10.0
1.0
0.1
0.01
mb/sr
(dσ/dΩ)lab
4 6 8 10 12 14 16 18 20 22 24 26 28 30 32 34
Z
XBL752-2301

Fig. 7b

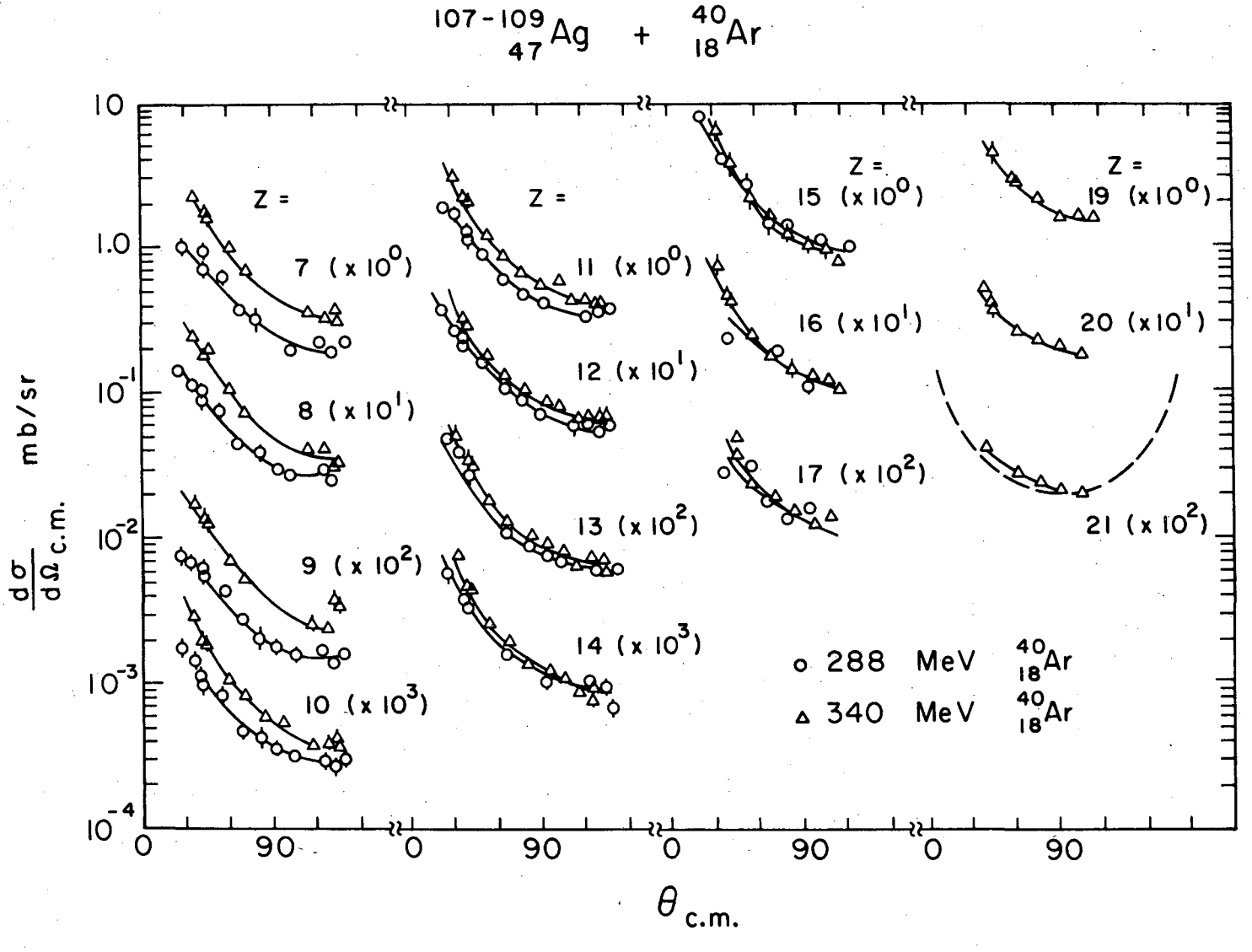

XBL752 - 2302

Fig. 8

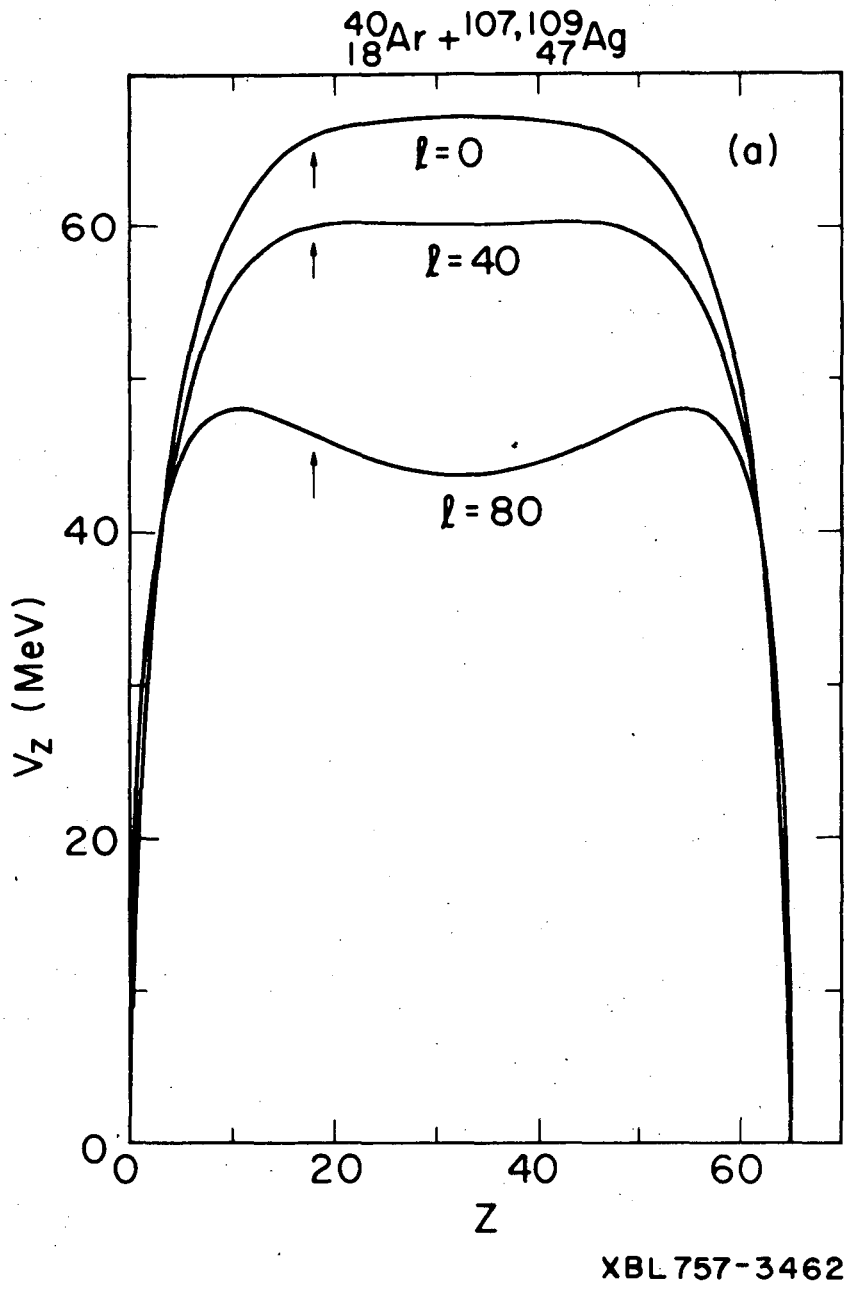

Fig. 9

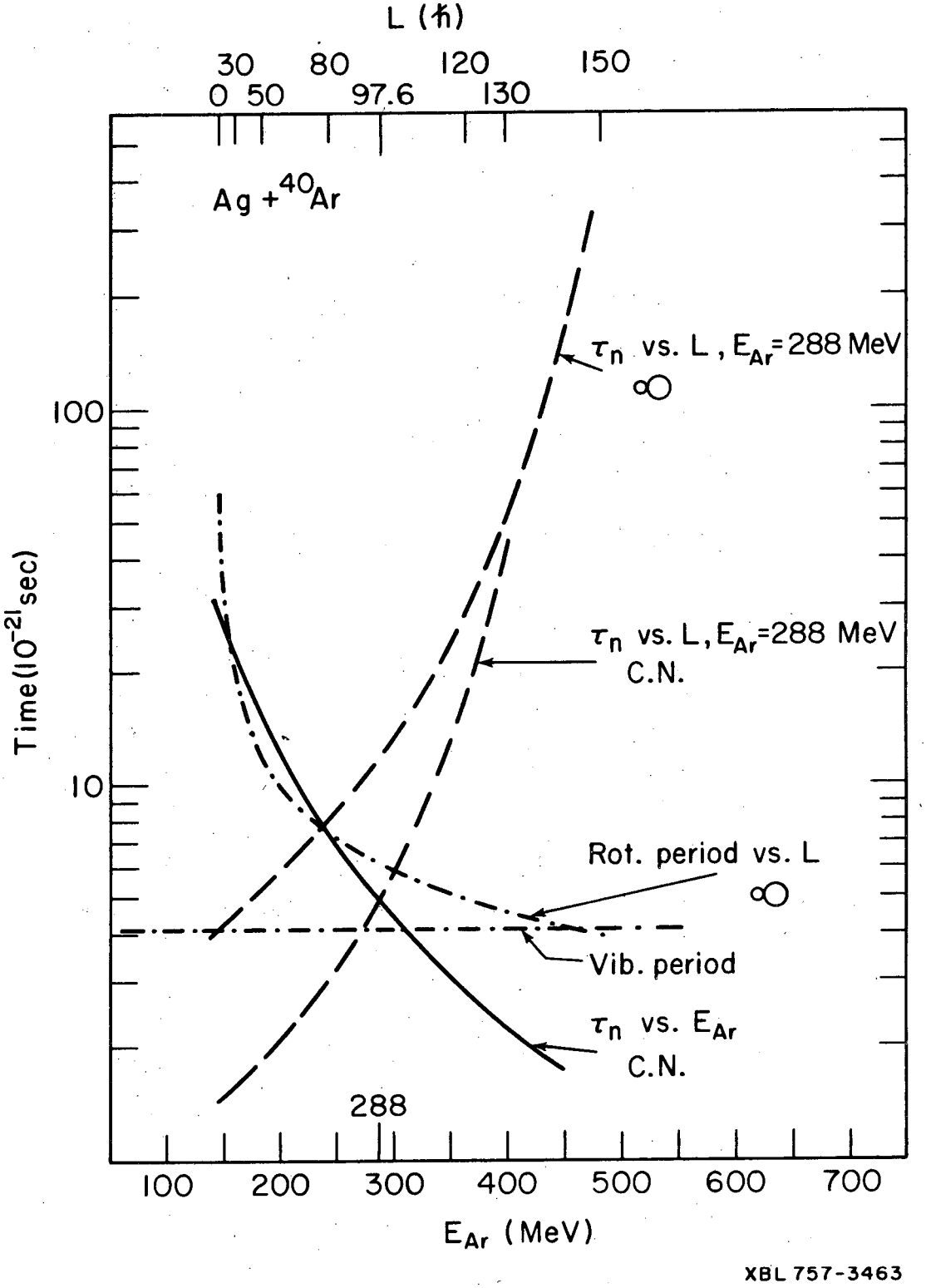
L (ħ)
30
80
120
150
0
50
97.6
130
Ag + 40Ar
τn vs. L, EAr=288 MeV
C.N.
τn vs. L, EAr=288 MeV
C.N.
Rot. period vs. L
Vib. period
τn vs. EAr
C.N.
Time(10-21 sec)
100
10
288
100
200
300
400
500
600
700
EAr (MeV)
XBL 757-3463

Fig. 10

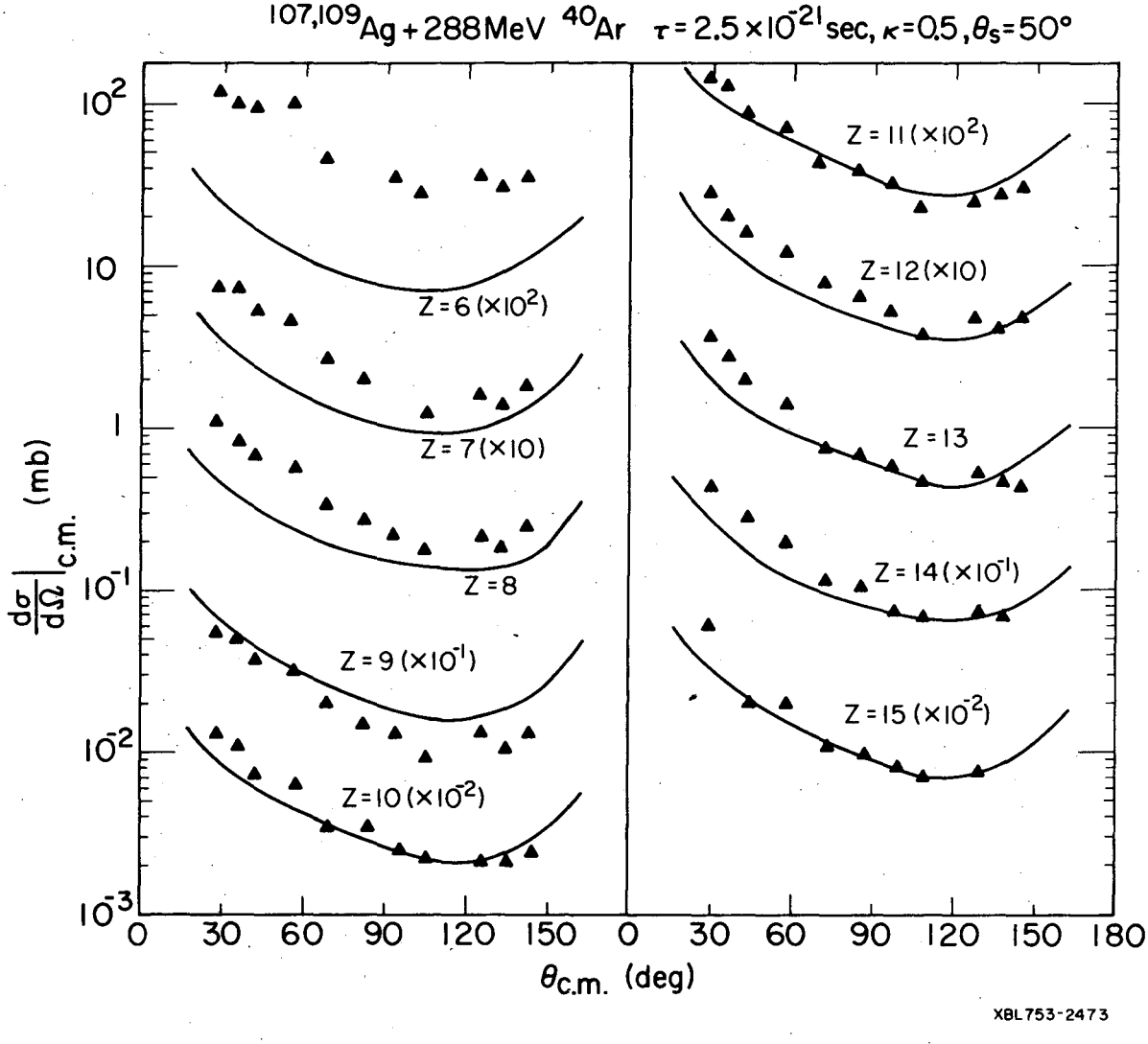
107,109Ag + 288MeV 40Ar τ = 2.5×10⁻²¹ sec, κ=0.5, θs=50°
dσ/dΩ|c.m. (mb)
θc.m. (deg)
Z = 6 (×10²)
Z = 7 (×10)
Z = 8
Z = 9 (×10⁻¹)
Z = 10 (×10⁻²)
Z = 11 (×10²)
Z = 12 (×10)
Z = 13
Z = 14 (×10⁻¹)
Z = 15 (×10⁻²)
XBL753-2473

Fig. 11

TECHNICAL INFORMATION DIVISION
LAWRENCE BERKELEY LABORATORY
UNIVERSITY OF CALIFORNIA
BERKELEY, CALIFORNIA 94720